Applied Catalysis B: Environmental 243 (2019) 455–462

Contents lists available at ScienceDirect

Applied Catalysis B: Environmental

journal homepage: www.elsevier.com/locate/apcatb

Microwave-assisted catalytic dehydration of glycerol for sustainable production of acrolein over a microwave absorbing catalyst

Qinglong Xie, Shanshan Li, Ruchao Gong, Gaoji Zheng, Yilei Wang, Pan Xu, Ying Duan, Shangzhi Yu, Meizhen Lu, Weirong Ji, Yong Nie*, Jianbing Ji

Biodiesel Laboratory of China Petroleum and Chemical Industry Federation, Zhejiang Provincial Key Laboratory of Biofuel, and College of Chemical Engineering, Zhejiang University of Technology, Hangzhou, 310014, China

ARTICLE INFO

Keywords:
Microwave
Dehydration
Glycerol
Acrolein
WO_3/ZrO_2@SiC catalyst

ABSTRACT

Uniform temperature distribution within solid catalyst particles is important to achieving low coke formation in a high-temperature reaction. However, the issue of uneven temperature distribution exists in most fixed-bed catalytic reaction systems. Here, we developed a microwave-assisted system and used it in catalytic dehydration of glycerol for sustainable production of acrolein. A coated microwave absorbing catalyst WO_3/ZrO_2@SiC was prepared and employed in the catalytic reactions. The effects of reaction temperature, ZrO_2/SiC ratio, and weight hourly space velocity (WHSV) on glycerol conversion and arcolein selectivity were examined. Experimental results showed that the microwave heating proved to be more effective than the conventional electric heating for glycerol dehydration to acrolein at lower temperature. The acrolein selectivity reached over 70% with complete glycerol conversion at 250 °C by microwave heating. The catalyst acidity was greatly influenced by ZrO_2/SiC ratio, which in turn determined the acrolein selectivity. More importantly, much better catalyst stability was obtained in the microwave-heating process than the electric-heating process. In addition, the microwave-heating system was effective for the *in-situ* regeneration of deactivated catalyst.

1. Introduction

Recently, increasing studies have been conducted on renewable energy, as a solution to current energy and environmental issues caused by traditional fossil fuels use. Biodiesel has attracted much interest as an alternative energy to non-renewable energy sources [1,2] since it is environmental friendly, technically feasible, and biodegradable [3]. Glycerol is the major by-product of biodiesel synthesis, which accounts for approximately 10 wt% of the total transesterification process production [4,5]. The tremendous increase in biodiesel production leads to a glut of glycerol in the market. The applications of glycerol to value-added chemicals have gained much attention, not only due to the surplus of glycerol available, but also because glycerol is edible, bio-sustainable, and non-toxic [6,7].

Glycerol has a wide variety of applications through different reaction pathways, due to its multi-functional structure and physico-chemical characteristics [8–10]. As one of the most important value-added chemicals that can be produced from glycerol, acrolein is a significant and flexible intermediate for the production of super-absorber polymers, detergents, textiles, and acrylic acid esters [11]. In addition, acrolein is utilized as the feedstock to produce DL-Methionine [12] and 1,3-propanediol [13] which are widely used in meat and material manufacturing, respectively.

Gas-phase catalytic dehydration of glycerol is widely considered as an economical and environmentally friendly approach to substitute conventional petrochemical process for acrolein production. Various types of catalysts were reported in previous studies on glycerol dehydration to acrolein, including heteropoly acids [14], zeolites [15], mixed metal oxides [16,17], phosphates [18], and pyrophosphates [19]. Particularly, metal oxide catalysts such as aluminum oxide (Al_2O_3) [20], niobium oxide (Nb_2O_5) [21], and tungsten oxide (WO_3) [22] have been widely used in acrolein production from glycerol and 60%–80% acrolein selectivity at almost complete glycerol conversion could be achieved. However, the main obstacle for industrial application of these catalysts is rapid deactivation due to coke formation on the catalyst surface [6,23]. The uneven temperature distribution within catalyst particles caused by conventional electric heating method is one of the most important reasons for the coke formation.

Microwave irradiation is an alternative heating method and has been successfully applied to many fields such as drying, food

* Corresponding author.
E-mail addresses: ny_zjut@zjut.edu.cn, nieyongnieyucheng@gmail.com (Y. Nie).

https://doi.org/10.1016/j.apcatb.2018.10.058
Received 9 June 2018; Received in revised form 20 October 2018; Accepted 24 October 2018
Available online 28 October 2018
0926-3373/

processing, and biomass pyrolysis and gasification [24–26]. Different from conventional heating processes where heat is transferred from the surface to the core of the material through conduction driven by temperature gradients, microwaves induce heat at the molecular level by direct conversion of electromagnetic energy into heat [27], and hence they can provide uniform internal heating for material particles. Therefore, microwave heating is expected to reduce the coke formation and improve the catalyst stability. In addition, the new heating method offers many other advantages over traditional processes, including simple set-up, rapid and convenient start-up and shut-down, and low cost [28]. However, no studies on glycerol dehydration to acrolein by microwave heating were reported.

A microwave heating and reaction system was previously developed by our group [29]. Using this system, microwave-assisted dehydration of glycerol for acrolein production over a novel coated microwave absorbing catalyst was conducted in this study. The effects of temperature, support coating to microwave absorbent ratio, and weight hourly space velocity (WHSV) on glycerol conversion and acrolein selectivity were investigated. The catalyst stability in microwave-heating and electric-heating processes was examined and compared. Moreover, microwave-assisted *in-situ* regeneration of deactivated catalyst was performed.

2. Experimental

2.1. Preparation of coated microwave absorbing catalyst

In this study, a coated microwave absorbing catalyst was used (some preliminary data on the superiority of coated catalyst over physically mixed catalyst are shown in Table S1 and Fig. S1). SiC with particle size of 500 nm was used as the microwave absorbent, whose temperature was increased very quickly when it absorbed the microwaves. A certain amount of SiC was dispersed in deionized water with liquid/solid ratio of 30 mL/g. Small amount of Na_2SiO_3 as dispersant was added to the SiC solution and kept under stirring at a temperature of 60 °C. Afterwards, an aqueous solution of $ZrOCl_2$ (10 wt%) was added at a constant flow rate of 2 mL/min, followed by the addition of diluted aqueous ammonia (ammonia/water ratio of 42.5 g/L) at a constant flow rate of 40 g/h. Once the addition of ammonia was completed the suspension was aged for 1 h at 60 °C while keeping the pH at 9.0–10.0. Subsequently, the precipitate was filtered, exhaustively washed with deionized water, dried in an oven at 105 °C for 12 h, and finally calcined under air flow at 550 °C for 3 h yielding the coated catalyst support designated as ZrO_2@SiC.

WO_3 was used as the active component of catalyst, which was loaded on the support using impregnation method. An aqueous solution of ammonia metatungstate (AMT) was added to ZrO_2@SiC powder kept under stirring at a temperature of 50 °C. Afterwards, the mixture was stirred for 6 h and aged for 12 h at the same temperature, followed by being dried in an oven at 105 °C for 12 h and calcined under air flow at 600 °C for 6 h yielding the coated microwave absorbing catalyst designated as WO_3/ZrO_2@SiC. The weight ratio of WO_3 to the whole catalyst was 10% in all the preparations. The schematic diagram of preparation of the WO_3/ZrO_2@SiC catalyst is shown in Fig. 1. Prior to use, the catalyst was ground, tabletted, crushed, and sieved to achieve a particle size of 0.85–1.00 mm.

2.2. Catalyst characterization

The Brunauer-Emmett-Teller (BET) specific surface area and pore size of catalysts were estimated from nitrogen adsorption-desorption isotherm data obtained at 77 K on a Micromeritics ASAP 2010 instrument. The samples were dehydrated under vacuum at 200 °C for 1 h prior to the nitrogen adsorption. The average pore diameter was calculated according to the Barret-Joyner-Hallender (BJH) method.

The powder X-ray diffraction (XRD) patterns, obtained on an X'Pert PRO (PANalytical) X-ray diffractometer instrument with a Cu–Kα radiation at 40 kV and 40 mA, were used to identify the major crystalline phases present in the catalysts and their crystallinity. Data collected from the instrument were analyzed using software MDI Jade 6.5.

The morphology of catalysts was observed by both scanning electron microscopy (SEM) and transmission electron microscopy (TEM) techniques. SEM images were acquired on an S-4700 (Hitachi) with the accelerating voltage at 15 kV. TEM and elemental mapping were performed on a Technai G2 F30 S-Twin (FEI) equipped with scanning TEM (STEM) accessories. The samples for TEM were prepared by ultrasonic dispersion of the catalyst in anhydrous ethanol and then loaded on a copper grid for testing.

The acid properties of catalysts were assessed by both temperature-programmed desorption of NH_3 (NH_3-TPD) and Fourier-transform infrared spectroscopy of pyridine (pyridine-FTIR) techniques. NH_3-TPD profiles were obtained in a DAS-7000 (Huasi Instruments, China) dynamic adsorption analyzer equipped with a thermal conductivity detector (TCD). Prior to ammonia adsorption, ca. 100 mg of sample was degassed under a 30 ml/min He flow at 200 °C for 1 h. After being cooled to 100 °C, the sample was saturated with anhydrous NH_3 at a flow rate of 30 ml/min for about 1 h. The sample was then purged with He to remove excess NH_3 from the sample surface. Finally, the TPD measurement was performed by heating the sample from 100 to 700 °C at a heating rate of 10 °C/min under a 30 ml/min He flow. In turn, pyridine-FTIR spectra were recorded in a Nicolet 380 FTIR apparatus for self-supported wafers (10 mg/cm^2) which were placed in an *in-situ* IR cell with a CaF_2 window and connected to a vacuum system. The wafer was dehydrated at 300 °C and dynamic vacuum of 10^{-4} Pa for 2 h. Afterwards, pyridine vapors were admitted to the IR cell at room temperature for 30 min and then the samples were degassed for 1 h at 200 °C or 350 °C. After each desorption step, the spectrum was recorded at room temperature with a resolution of 4.0 cm^{-1} and the background was subtracted.

Thermogravimetry-differential scanning calorimetry (TG-DSC) measurements were performed in a TGA/DSC 1/1600 H T (Mettler-Toledo) simultaneous thermal analyzer. Dry air provided by a pressured tank with a flow rate of 50 ml/min was used as the carrier gas. The

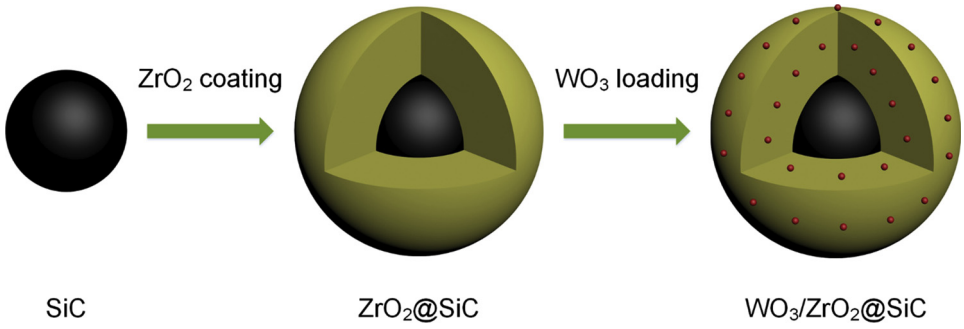

Fig. 1. Schematic diagram of preparation of coated microwave absorbing catalyst WO_3/ZrO_2@SiC.

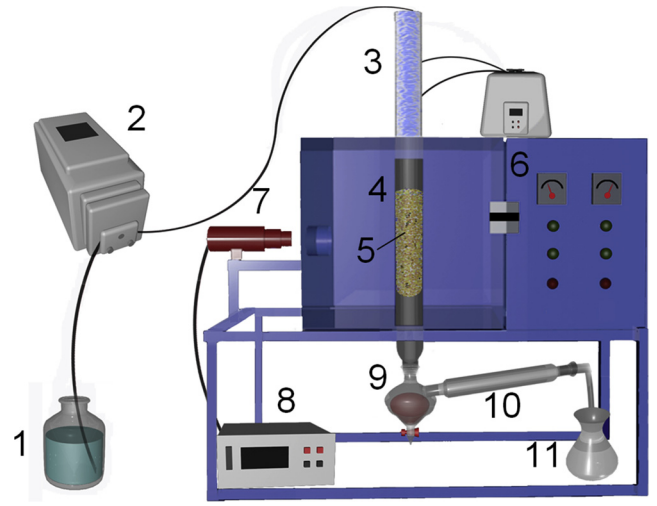

Fig. 2. Schematic diagram of microwave-assisted catalytic dehydration of glycerol for acrolein production. (1) Feedstock bottle; (2) peristaltic pump; (3) preheater; (4) quartz reactor; (5) catalyst bed; (6) microwave oven; (7) infrared radiation thermometer (SS100, Kentech) to measure the temperature of catalyst bed; (8) temperature recorder and controller; (9) liquid product flask; (10) condenser; (11) water seal.

baseline was subtracted from a blank run. Catalyst and reference alumina samples were loaded into twin holders. The measurements were carried out from room temperature to 800 °C at a heating rate of 10 °C/min.

2.3. Catalytic tests

Glycerol dehydration tests were performed in a self-designed microwave oven (manufactured by Chenou Microwave Equipment Corporation, Jiangyin, China), with the power of 800 W at a microwave frequency of 2450 MHz. The schematic diagram of experimental apparatus is shown in Fig. 2. For safety purpose, a microwave detector (DT-2 G, CEM Corporation) was used to monitor microwave leakage.

A vertical fixed-bed quartz reactor with an inner diameter of 20.0 mm was used in this study, For each test, 14.0 g of catalyst without diluents was loaded in the middle of the reactor with quartz wool packed in both ends. In order to remove the air within the reactor, N_2 was introduced into the system at a flow rate of 30 ml/min for 30 min prior to the commencement of microwave heating. The microwave oven was then turned on for heating process. When the temperature of catalyst bed reached the reaction temperature, aqueous glycerol (20% wt/wt) was fed to the reactor by a peristaltic pump, which was preheated and gasified before entering the reactor. At the same time, the microwave oven was controlled to be on or off in order to maintain a stable temperature of the catalyst bed, with the deviation of temperature measured by an infrared radiation thermometer within ± 1 °C. Flowing through the condenser, the condensable components were condensed and collected as the liquid product for subsequent analysis. The yield of liquid product was calculated using Eq. (1).

$$\text{Liquid product yield(wt\%)} = \frac{\text{The weight of liquid product}}{\text{The weight of feedstock}} \times 100\% \quad (1)$$

The dehydration of glycerol was also conducted using conventional electric heating method to compare with the microwave heating method. The experimental apparatus and process were basically the same, except for the heating device changed from the microwave oven to an electric heating unit with the temperature monitored by a thermocouple placed on the outer wall of the reactor.

2.4. Product analysis

Glycerol in the liquid product was analyzed using a Shimadzu LC-20AT high performance liquid chromatography (HPLC) with a XAmide column (150 mm × 4.6 mm, 5 μm) and a refractive index detector (RID). A mixture of acetonitrile and water (90:10) was used as the mobile phase at a flow rate of 0.8 mL/min. The injection size was 20 μl and oven temperature was kept at 35 °C. External standard method was used for glycerol quantification. The glycerol conversion was determined using Eq. (2).

$$\text{Glycerol conversion}(\%) = \left(1 - \frac{\text{The amount of glycerol in liquid product}}{\text{The amount of glycerol in feedstock}}\right) \times 100\% \quad (2)$$

Acrolein and by-products (mainly acetaldehyde and hydroxyacetone) in the liquid product were determined using an Agilent 7890 A gas chromatography (GC) equipped with a DB-WAX capillary column (30 m × 0.32 mm × 0.50 μm) and a flame ionization detector (FID). Since the large amount of water in the liquid product would damage the column and detector, chloroform was used to extract acrolein from the liquid product for subsequent GC analysis. Nitrogen was used as the carrier gas at a flow rate of 30 mL/min. The flow rates of hydrogen and air were 30 and 300 mL/min, respectively. The injection size was 1 μl with a split ratio of 1:30. The oven temperature was 40 °C initially held for 6 min and then increased to 60 °C at a heating rate of 5 °C/min, followed by increase to 220 °C at a heating rate of 15 °C/min and being held at 220 °C for 10 min. The temperatures of injector and detector were maintained at 250 °C and 300 °C, respectively. Internal standard method was used for products quantification with methanol as the internal standard. The selectivity and yield of products were calculated using Eqs. (3) and (4). The data shown in this study are the averaged values in the range of 4–6 h on stream, with the results representing stable glycerol conversion and products selectivity.

$$\text{Product selectivity}(\%) = \frac{\text{The amount of glycerol converted to a product}}{\text{The amount of reacted glycerol}} \times 100\% \quad (3)$$

$$\text{Product yield}(\%) = \frac{\text{The amount of glycerol converted to a product}}{\text{The amount of glycerol in feedstock}} \times 100\% \quad (4)$$

3. Results and discussion

3.1. Characterization of the catalysts

The specific surface area of the microwave absorbent SiC was only 13 m^2/g, making it unsuitable to be catalyst support. For the coated catalyst support ZrO_2@SiC prepared in this study, the ZrO_2 coating with certain pore channel and structure obviously increased the specific surface area (55–65 m^2/g), which could improve the loading of active component WO_3.

The powder XRD patterns of the WO_3/ZrO_2@SiC catalysts with various ZrO_2/SiC weight ratios are shown in Fig. S2. The characteristic peaks of SiC, ZrO_2 and WO_3 were observed for all the catalysts, indicating the existence of corresponding crystalline phases in the catalysts. The crystalline sizes of WO_3, as estimated by the Scherrer equation, were 8–14 nm for catalysts with different ZrO_2/SiC ratios, which revealed good dispersion of WO_3 on the ZrO_2 coating.

The SEM images of the WO_3/ZrO_2@SiC catalysts with various ZrO_2/SiC weight ratios are displayed in Fig. S3. All the samples showed platelet-shaped microstructures with each "platelet" covered with smaller particles. It can be confirmed by the TEM images of the WO_3/ZrO_2@SiC catalysts as shown in Figs. 3a and S4. Fig. 3b displays a high resolution TEM image of the typical WO_3/ZrO_2@SiC sample with ZrO_2/

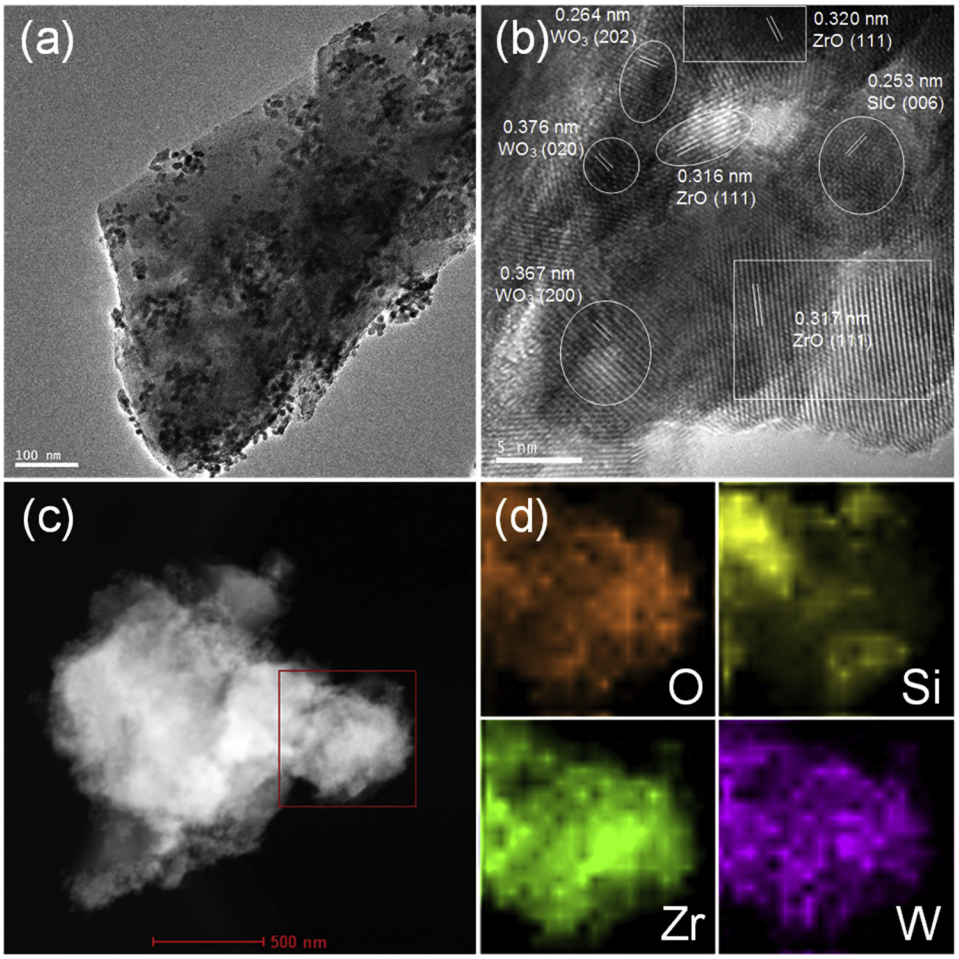

Fig. 3. (a) TEM, (b) HR-TEM, and (c) HAADF-STEM images of the typical WO_3/ZrO_2@SiC catalyst with ZrO_2/SiC weight ratio of 3:5 and the corresponding (d) elemental mapping from (c). In (c), the red rectangle is the area for elemental mapping (For interpretation of the references to colour in this figure legend, the reader is referred to the web version of this article).

SiC weight ratio of 3:5. Clearly, we can observe the lattice fringes of SiC (0 0 6), ZrO_2 (1 1 1) and WO_3 (0 2 0), (2 0 0), (2 0 2). The elemental mapping was then acquired using high-angle annular dark-field STEM (HAADF-STEM) with energy dispersive X-ray spectrometer (EDX). As shown in Figs. 3c and d, uniform distributions of O, Si, Zr and W were found. Similar profiles for the WO_3/ZrO_2@SiC catalysts with ZrO_2/SiC weight ratio of 1:3, 1:1 and 5:3 were also demonstrated (Fig. S5).

NH_3-TPD was carried out to determine the acidity of the WO_3/ZrO_2@SiC catalysts. As shown in Fig. 4, all the samples featured a main desorption peak at higher temperature attributed to relatively strong acid sites, along with a lower-temperature shoulder assigned to weak acid sites. However, a shift in the maximum peak position in both low- and high-temperature regions was observed for catalysts with different ZrO_2/SiC ratios, which was mainly due to the change in surface acid strength resulting from the change in relative contents of ZrO_2 and WO_3.

The FTIR spectra after pyridine desorption at 200 °C and 350 °C were recorded respectively to determine the amounts of Brønsted and Lewis acid sites on the catalysts. As shown in Figs. 5 and S6, similar FTIR profiles and desorption peaks were observed at both desorption temperatures. Typical bands due to the vibration mode of pyridine protonated by Brønsted acid sites (pyridinium ions, PyH^+) appeared at ca. 1546 and 1640 cm^{-1} [30]. Pyridine coordinated to the Lewis acid sites (coordinatively unsaturated Al^{3+}, PyL) exhibited bands centered at 1445–1446, 1449–1455, ca. 1597 and 1624 cm^{-1} [30]. The band centered at 1491 cm^{-1} was attributed to the combination of Brønsted and Lewis acid sites [31].

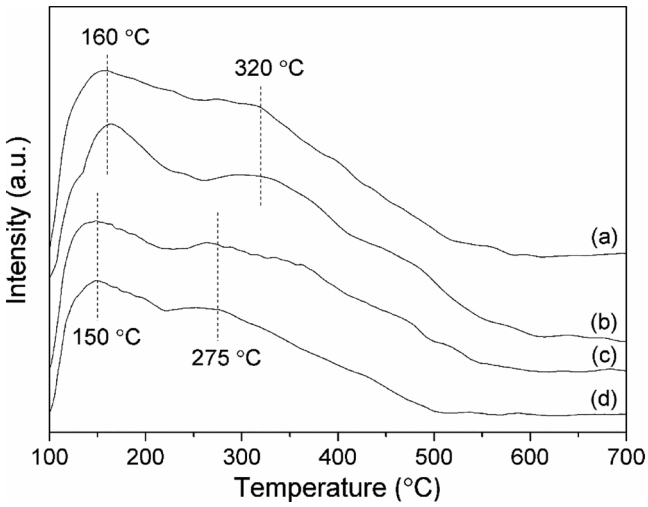

Fig. 4. NH_3-TPD profiles of the WO_3/ZrO_2@SiC catalysts with ZrO_2/SiC weight ratios of (a) 1:3, (b) 3:5, (c) 1:1, and (d) 5:3.

The density of acid sites on the catalysts as determined by NH_3-TPD and pyridine-FTIR techniques is listed in Table 1. The total amount of acid sites first increased and then decreased with an increase in the ZrO_2 content. The largest amounts of weak, strong and total acid sites were observed when the ZrO_2/SiC weight ratio was 3:5. The amounts of

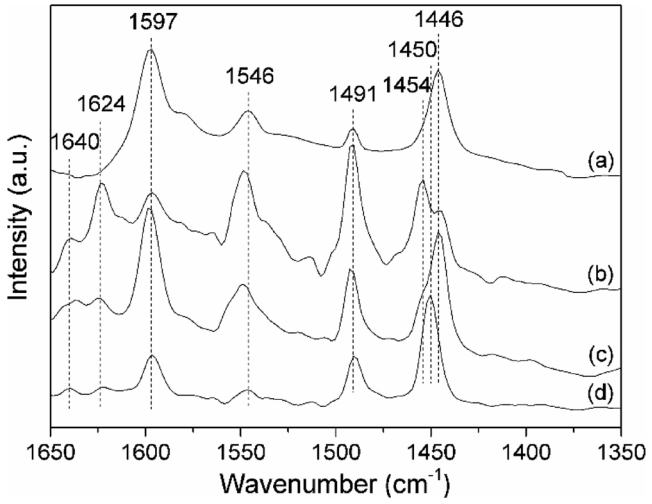

Fig. 5. Pyridine-FTIR profiles at a desorption temperature of 200 °C of the WO_3/ZrO_2@SiC catalysts with ZrO_2/SiC weight ratios of (a) 1:3, (b) 3:5, (c) 1:1, and (d) 5:3.

Brønsted and Lewis acid sites were calculated from the integrated areas of the corresponding bands using the extinction coefficients reported by Emeis [32]. A large amount of Lewis acid sites were observed when the ZrO_2/SiC ratio was too low or too high. The highest ratio of Brønsted acid density to Lewis acid density was obtained at the ZrO_2/SiC weight ratio of 3:5.

3.2. Effect of reaction temperature

The effect of reaction temperature on glycerol conversion and acrolein selectivity in microwave-assisted glycerol dehydration is shown in Table 2. It can be seen that the liquid product yield was approximately 100% when the temperature was higher than 230 °C, meaning that few gaseous products, such as CO or CO_2 which can be easily produced in the presence of oxygen [33,34], formed under the anaerobic condition in this study. The low liquid product yield, glycerol conversion and acrolein selectivity obtained at 210 °C was mainly because the aqueous glycerol was not completely converted or even gasified at this temperature and some glycerol might remain on the catalyst bed or on the reactor wall.

As shown in Table 2, complete glycerol conversion was observed when the reaction temperature was higher than 250 °C. Since secondary cracking reactions were improved by higher temperature, an increase in the yield of acetaldehyde was found with increasing temperature. Smaller molecules enhanced the formation of carbon deposit, reducing the acrolein selectivity and catalyst stability. In addition, the formation of dimers and polymers which were derived from acrolein, acetaldehyde and hydroxyacetone, such as polyacrolein, would be improved at higher temperature. On the other hand, it is probably that more by-products other than acetaldehyde and hydroxyacetone, e.g., polyglycerol, were produced at lower temperature, which would result in a lower acrolein yield. Overall, the optimal temperature for acrolein production from microwave-assisted catalytic dehydration of glycerol was 250–270 °C, at which the acrolein yield reached over 70%.

Table 2
Effect of reaction temperature on microwave-assisted catalytic dehydration of glycerol[a].

Temperature (°C)	210	230	250	270	290
Liquid product yield (wt%)	93.3	97.2	98.0	97.7	97.9
Glycerol conversion (%)	45.3	90.8	100	100	100
Products selectivity (%)					
Acrolein	29.1	65.7	71.1	70.4	67.8
Acetaldehyde	0.04	0.1	0.7	1.3	1.1
Hydroxyacetone	3.1	7.1	8.1	6.1	7.7
Others[b]	67.7	27.1	20.1	22.2	23.4

[a] Reaction conditions: feed composition: 20 wt% glycerol, 80 wt% H_2O; WHSV = 1.0 h^{-1}; ZrO_2/SiC ratio (wt/wt) was 3:5.
[b] Selectivity for other products mainly including dimers and polymers which were derived from glycerol, acrolein, acetaldehyde and hydroxyacetone (%) = 100 – Σ(selectivity for each identified product listed).

For comparison, the glycerol dehydration to acrolein was also conducted using conventional electric heating method. As displayed in Table 3, the reaction temperature exhibited similar effect on the electric-heating glycerol dehydration to the microwave-heating process. However, much lower glycerol conversion and acrolein selectivity was obtained at 250 °C in the electric-heating process than that under the same conditions in the microwave-heating process. The glycerol conversion reached over 95% only when the temperature was higher than 310 °C. It was mainly because the glycerol dehydration is an endothermic reaction, with some heat in the system continuously carried away during the process. For the conventional electric heating, heat was transferred from the reactor wall to the catalyst bed through conduction, which easily caused temperature gradients resulting in a lower temperature in the interior of the catalyst bed. By contrast, microwaves provided uniform internal heating by direct conversion of the electromagnetic energy into heat at the molecular level. From the comparison between the electric-heating and microwave-heating processes (Tables 2 and 3), we can find at least 40–60 °C temperature gradient existed within the catalyst bed during the electric-heating reaction, which would increase the coke formation and hence catalyst deactivation rate.

Table 1
Acidity of the WO_3/ZrO_2@SiC catalysts with various ZrO_2/SiC weight ratios, as determined by NH_3-TPD and pyridine-FTIR techniques.

ZrO_2/SiC (wt/wt)	Density of acid sites by NH_3-TPD (μmol $NH_3/g_{cat.}$)			Density of acid sites by pyridine-FTIR (μmol/$g_{cat.}$)					
	Weak[a]	Strong[a]	Total[a]	B200[b]	L200[b]	B200/L200	B350[b]	L350[b]	B350/L350
1:3	285	300	585	6	116	0.05	4	80	0.05
3:5	486	570	1056	44	46	0.96	39	40	0.98
1:1	222	370	592	12	52	0.23	10	27	0.37
5:3	245	334	579	12	89	0.13	8	48	0.17
Stability[c]	469	557	1026	42	41	1.02	37	35	1.06
Deactivated[d]	124	146	270	4	22	0.18	2	19	0.11
Regenerated[e]	438	524	962	42	39	1.08	36	24	1.50

[a] Weak: weak acid sites; strong: strong acid sites; and total: total acid sites.
[b] B: Brønsted acid sites; and L: Lewis acid sites. The number after B or L refers to the pyridine desorption temperature (in °C).
[c] Stability refers to the WO_3/ZrO_2@SiC catalyst (ZrO_2/SiC weight ratio was 3:5) after 24 h continuous run at 250 °C in the microwave-heating process.
[d] Deactivated refers to the WO_3/ZrO_2@SiC catalyst (ZrO_2/SiC weight ratio was 3:5) after 24 h continuous run at 250 °C in the electric-heating process.
[e] Regenerated refers to the WO_3/ZrO_2@SiC catalyst (ZrO_2/SiC weight ratio was 3:5) after microwave-assisted *in-situ* regeneration.

Table 3
Effect of reaction temperature on catalytic dehydration of glycerol using electric heating[a].

Temperature (°C)	250	270	290	310	330	350
Liquid product yield (wt%)	97.8	98.4	96.5	95.2	96.4	98.6
Glycerol conversion (%)	83.8	85.9	92.8	95.0	96.8	97.4
Products selectivity (%)						
Acrolein	53.5	61.8	62.2	61.5	66.5	69.0
Acetaldehyde	0.1	0.3	0.4	0.9	0.9	0.5
Hydroxyacetone	5.8	9.0	7.8	4.0	4.2	6.2
Others[b]	40.6	28.9	29.6	33.6	28.4	24.2

[a] Reaction conditions: feed composition: 20 wt% glycerol, 80 wt% H_2O; WHSV = 1.0 h^{-1}; ZrO_2/SiC ratio (wt/wt) was 3:5.
[b] Selectivity for other products mainly including dimers and polymers which were derived from glycerol, acrolein, acetaldehyde and hydroxyacetone (%) = 100 – Σ(selectivity for each identified product listed).

3.3. Effect of ZrO2/SiC ratio

ZrO_2/SiC ratio was an important factor influencing catalytic performance of the WO_3/ZrO_2@SiC catalyst. SiC as the core was used to absorb the microwaves and provide even temperature distribution by means of the unique heating characteristics and mechanism of the microwave technique. On the other hand, ZrO_2 coating provided large specific surface area for WO_3 loading. More importantly, the interaction of ZrO_2 with WO_3 could influence and even determine the catalyst acidity which had crucial effect on the acrolein selectivity [16].

As shown in Table 4, the highest and the lowest acrolein selectivity were obtained at the ZrO_2/SiC weight ratio of 3:5 and 1:3, respectively. The results can be well explained by the acidity of catalysts with different ZrO_2/SiC ratios as listed in Table 1. The effect of catalyst acidity on products selectivity was realized through two aspects, i.e., the strength of acidity [35] and the type of acid sites [36]. Stronger acid sites were reported to be more active than weaker acid sites for the production of acrolein [23,37–39]. On the other hand, it was widely accepted that Brønsted acid sites appeared more effective than Lewis acid sites in promoting the selective formation of acrolein [12,40–42]. As seen in Table 1, the catalyst with ZrO_2/SiC weight ratio of 3:5 possessed the highest density of strong and Brønsted acid sites, which resulted in the highest acrolein selectivity. The highest selectivity to the by-product hydroxyacetone was obtained over the same catalyst, probably due to the highest density of weak acid sites [43].

3.4. Effect of WHSV

Change in WHSV was realized by adjusting the feeding rate of glycerol aqueous solution and keeping the weight of catalyst constant. As shown in Table 5, the glycerol conversion decreased with increasing WHSV especially when the WHSV was higher than 2.5 h^{-1}. Some glycerol might remain on the catalyst bed when the feeding rate was too high, which led to a decrease in liquid product yield.

Table 4
Effect of ZrO_2/SiC ratio on microwave-assisted catalytic dehydration of glycerol[a].

ZrO_2/SiC ratio (wt/wt)	1:3	3:5	1:1	5:3
Liquid product yield (wt%)	95.4	98.0	94.0	94.5
Glycerol conversion (%)	99.9	100	100	100
Products selectivity (%)				
Acrolein	53.7	71.1	62.8	68.3
Acetaldehyde	2.6	0.7	0.6	0.7
Hydroxyacetone	4.8	8.1	7.0	5.7
Others[b]	38.9	20.1	29.6	25.3

[a] Reaction conditions: feed composition: 20 wt% glycerol, 80 wt% H_2O; reaction temperature was 250 °C; WHSV = 1.0 h^{-1}.
[b] Selectivity for other products mainly including dimers and polymers which were derived from glycerol, acrolein, acetaldehyde and hydroxyacetone (%) = 100 – Σ(selectivity for each identified product listed).

Table 5
Effect of WHSV on microwave-assisted catalytic dehydration of glycerol[a].

WHSV (h^{-1})	0.5	1.0	2.5	5.0
Liquid product yield (wt%)	96.3	98.0	96.9	95.0
Glycerol conversion (%)	98.8	100	91.8	73.5
Products selectivity (%)				
Acrolein	62.2	71.1	60.8	58.8
Acetaldehyde	0.3	0.7	0.5	0.6
Hydroxyacetone	7.5	8.1	9.0	11.3
Others[b]	30.0	20.1	29.7	29.3

[a] Reaction conditions: feed composition: 20 wt% glycerol, 80 wt% H_2O; reaction temperature was 250 °C; ZrO_2/SiC ratio (wt/wt) was 3:5.
[b] Selectivity for other products mainly including dimers and polymers which were derived from glycerol, acrolein, acetaldehyde and hydroxyacetone (%) = 100 – Σ(selectivity for each identified product listed).

Products selectivity was also influenced by WHSV. It is generally accepted that glycerol undergoes two steps of dehydration to form acrolein [44,45], and hence acrolein production would be hindered when WHSV was too high. The low acrolein selectivity at the WHSV of 0.5 h^{-1} was probably caused by the side reactions including secondary cracking reactions and recombination of smaller molecules which would increase the carbon deposit on catalyst and could be enhanced by low WHSV or long residence time. In addition, the increase in WHSV favored the production of hydroxyacetone. Overall, the optimal WHSV was around 1.0 h^{-1} for the WO_3/ZrO_2@SiC catalyst.

3.5. Catalyst stability

The catalyst stability in both microwave-heating and electric-heating glycerol dehydration to acrolein was examined through continuous run for 24 h. As shown in Fig. 6, the glycerol conversion remained almost unchanged during the entire process and the value was still higher than 97.5% even after 24 h run. In addition, stable acrolein selectivity with time on stream was observed, mostly in the range of 60%–70%. It demonstrated that the WO_3/ZrO_2@SiC catalyst had good stability in the microwave-assisted glycerol dehydration process. Moreover, little change in the density of acid sites on the catalyst after the stability test was observed, as shown in Table 1. The performance

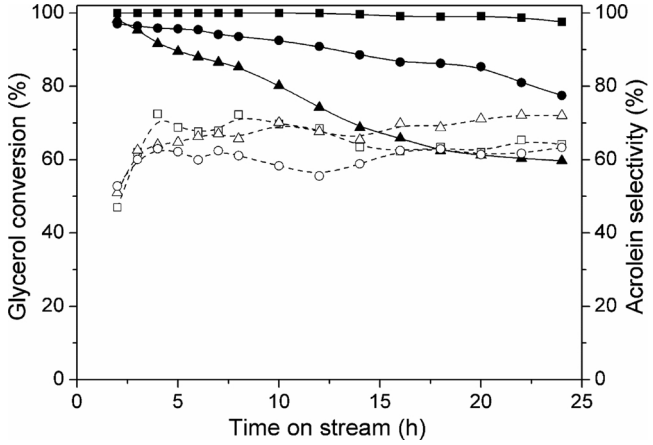

Fig. 6. Glycerol conversion (filled symbols with solid lines) and acrolein selectivity (open symbols with dash lines) with time on stream in microwave-heating and electric-heating catalytic dehydration of glycerol. Reaction conditions: feed composition: 20 wt% glycerol, 80 wt% H_2O; reaction temperature: (■) 250 °C by microwave heating, (▲) 250 °C by electric heating, and (●) 310 °C by electric heating; WHSV = 1.0 h^{-1}; ZrO_2/SiC ratio (wt/wt) was 3:5.

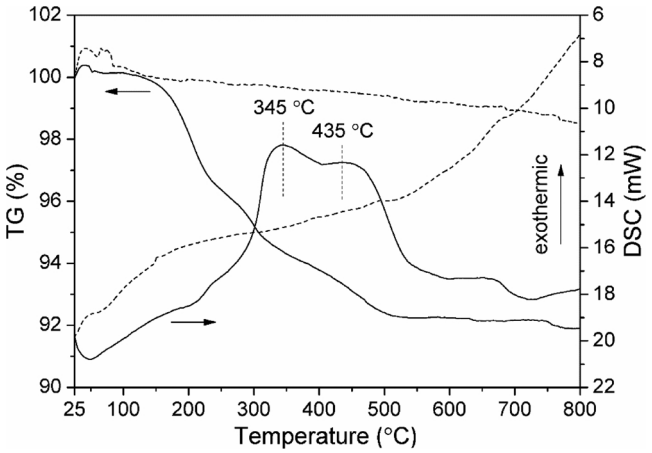

Fig. 7. TG-DSC curves of the used (solid lines) and fresh (dash lines) WO_3/ZrO_2@SiC catalyst.

was better than that in the electric-heating process and those in many previous studies [20,23,34,46]. It was mainly attributed to the even temperature distribution within the catalyst bed which resulted from the uniform internal heating provided by microwave irradiation.

By contrast, obvious catalyst deactivation was found in the glycerol dehydration using conventional electric heating and even more rapid catalyst deactivation was observed at lower temperature, even though the acrolein selectivity was still stable during the entire process. Similar results were obtained at some previously reported zirconia-supported tungsten oxide (or tungstated zirconia, WO_3/ZrO_2) catalysts [16,22,47,48]. One important reason for the rapid catalyst deactivation lied in the temperature gradient within the catalyst bed which would promote the formation of by-products and precursors of carbonaceous deposits.

NH_3-TPD and pyridine-FTIR of the WO_3/ZrO_2@SiC catalyst after 24 h continuous run at 250 °C in the electric-heating process were conducted to assess the acid properties of deactivated catalyst. As shown in Table 1, the density of acid sites on the deactivated catalyst was significantly decreased compared with the fresh one, especially the Brønsted acid sites. It suggested that the surface carbonaceous deposits were likely to be adsorbed on the acid sites on the WO_3/ZrO_2@SiC catalyst, weakening its acidity to favor glycerol activation for selective dehydration to form acrolein. TG-DSC curves of the used and fresh WO_3/ZrO_2@SiC catalyst (Fig. 7) revealed that at least two types of surface carbonaceous deposits, corresponding to the DSC peaks of the used catalyst at 345 °C and 435 °C, respectively, existed on the deactivated catalyst from the electric-heating process.

3.6. Catalyst regeneration

As shown in Fig. 7, the TG curve of the used catalyst was almost unchanged when the temperature was higher than 500 °C, indicating most carbonaceous deposits could be removed at 500 °C. Therefore, microwave-assisted *in-situ* regeneration of the deactivated catalyst was conducted on the same microwave system. The catalyst bed was first heated by microwaves under a 30 ml/min N_2 flow which was changed to 20 ml/min air flow when the temperature reached 500 °C. After being activated for 1 h, the catalyst was exposed to 40 ml/min air flow for another 1 h to guarantee the removal of most carbonaceous deposits from the catalyst.

The regenerated catalyst was then tested in microwave-assisted glycerol dehydration at 250 °C for acrolein production. The glycerol conversion and acrolein selectivity reached 97.9% and 64.1%, respectively, which were slightly lower than those obtained over fresh catalyst. NH_3-TPD and pyridine-FTIR results (Table 1) revealed that most acid sites, especially strong and Brønsted acid sites which favored the selective formation of acrolein, were recovered during the regeneration process. Therefore, the microwave-heating process and system proved to be effective for the *in-situ* regeneration of deactivated catalyst, which provided a reference for continuous and even industrial production of acrolein.

4. Conclusions

In this study, microwave-assisted catalytic dehydration of glycerol for sustainable acrolein production over a coated microwave absorbing catalyst WO_3/ZrO_2@SiC was investigated. Microwave heating provided more even temperature distribution within the catalyst bed than conventional electric heating, resulting in higher acrolein yield at lower temperature and better catalyst stability. The technique of microwave heating coupled with microwave absorbing catalyst provides a novel and effective method for the research on and even scale up of sustainable production of acrolein.

Acknowledgements

The authors would like to express their great appreciation to the National Natural Science Foundation of China (21808203) and the Natural Science Foundation of Zhejiang Province (LQ17B060003) for their financial support for this work.

Appendix A. Supplementary data

Supplementary material related to this article can be found, in the online version, at doi:https://doi.org/10.1016/j.apcatb.2018.10.058.

References

[1] M. Hajjari, M. Tabatabaei, M. Aghbashlo, H. Ghanavati, A review on the prospects of sustainable biodiesel production: A global scenario with an emphasis on waste-oil biodiesel utilization, Renew. Sus. Energy Rev. 72 (2017) 445–464.
[2] S.S. Prabu, M.A. Asokan, R. Roy, S. Francis, M.K. Sreelekh, Performance, combustion and emission characteristics of diesel engine fuelled with waste cooking oil biodiesel/diesel blends with additives, Energy 122 (2017) 638–648.
[3] H.M. Mahmudul, F.Y. Hagos, R. Mamat, A.A. Adam, W.F.W. Ishak, R. Alenezi, Production, characterization and performance of biodiesel as an alternative fuel in diesel engines – a review, Renew. Sustain. Energy Rev. 72 (2017) 497–509.
[4] M. Pagliaro, R. Ciriminna, H. Kimura, M. Rossi, C.D. Pina, From glycerol to value-added products, Angew. Chem. Int. Ed. 46 (2007) 4434–4440.
[5] B. Katryniok, S. Paul, F. Dumeignil, Recent developments in the field of catalytic dehydration of glycerol to acrolein, ACS Catal. 3 (2013) 1819–1834.
[6] H. Park, Y.S. Yun, T.Y. Kim, K.R. Lee, J. Baek, J. Yi, Kinetics of the dehydration of glycerol over acid catalysts with an investigation of deactivation mechanism by coke, Appl. Catal. B-Environ. 176 (2015) 1–10.
[7] Q. He, J. McNutt, J. Yang, Utilization of the residual glycerol from biodiesel production for renewable energy generation, Renew. Sustain. Energy Rev. 71 (2017) 63–76.
[8] C.W. Chiu, M.J. Goff, G.J. Suppes, Distribution of methanol and catalysts between biodiesel and glycerin phases, AlChE J. 51 (2005) 1274–1278.
[9] M. di Serio, L. Casale, R. Tesser, E. Santacesaria, Development of a process for the acid-catalyzed etherification of glycerine and isobutene forming glycerine tertiary butyl ethers, Energy Fuel 24 (2010) 4668–5467.
[10] H.W. Tan, A.R.A. Aziz, M.K. Arona, Glycerol production and its applications as a raw material: a review, Renew. Sus. Energy Rev. 27 (2013) 118–127.
[11] X. Fan, R. Burton, Y. Zhou, Glycerol (byproduct of biodiesel production) as a source for fuels and chemicals – mini review, Open Fuel Energy Sci. J. 3 (2010) 17–22.
[12] B. Katryniok, S. Paul, V. Bellière-Beca, P. Rey, F. Dumeignil, Glycerol dehydration to acrolein in the context of new uses of glycerol, Green Chem. 12 (2010) 2079–2098.
[13] M. Watanabe, T. Iida, Y. Aizawa, T.M. Aida, H. Inomata, Acrolein synthesis from glycerol in hot-compressed water, Bioresour. Technol. 98 (2007) 1285–1290.
[14] T.H. Kang, J.H. Choi, Y. Bang, J. Yoo, J.H. Song, W. Joe, J.S. Choi, I.K. Song, Dehydration of glycerin to acrolein over $H_3PW_{12}O_{40}$ heteropolyacid catalyst supported on silica-alumina, J. Mol. Catal. A-Chem. 396 (2015) 282–289.
[15] H.P. Decolatti, B.O.D. Costa, C.A. Querini, Dehydration of glycerol to acrolein using H-ZSM5 zeolite modified by alkali treatment with NaOH, Microporous Mesoporous Mater. 204 (2015) 180–189.
[16] S. Chai, B. Yan, L. Tao, Y. Liang, B. Xu, Sustainable production of acrolein: catalytic gas-phase dehydration of glycerol over dispersed tungsten oxides on alumina, zirconia and silica, Catal. Today 234 (2014) 215–222.
[17] C. Garcia-Sancho, J.A. Cecilia, J.M. Merida-Robles, J.S. Gonzalez, R. Moreno-Tost, A. Infantes-Molina, P. Maireles-Torres, Effect of the treatment with H_3PO_4 on the

catalytic activity of Nb_2O_5 supported on Zr-doped mesoporous silica catalyst. Case study: glycerol dehydration, Appl. Catal. B-Environ. 221 (2018) 158–168.
[18] Y. Choi, D.S. Park, H.J. Yun, J. Baek, D. Yun, J. Yi, Mesoporous siliconiobium phosphate as a pure brønsted acid catalyst with excellent performance for the dehydration of glycerol to acrolein, ChemSusChem 5 (2012) 2460–2468.
[19] X. Feng, Y. Yao, Q. Su, L. Zhao, W. Jiang, W. Ji, C.T. Au, Vanadium pyrophosphate oxides: The role of preparation chemistry in determining renewable acrolein production from glycerol dehydration, Appl. Catal. B-Environ. 164 (2015) 31–39.
[20] Y.T. Kim, K.D. Jung, E.D. Park, Gas-phase dehydration of glycerol over silica-alumina catalysts, Appl. Catal. B-Environ. 107 (2011) 177–187.
[21] C. Garcia-Sancho, J.A. Cecilia, A. Moreno-Ruiz, J.M. Merida-Robles, J. Santamaria-Gonzalez, R. Moreno-Tost, P. Maireles-Torres, Influence of the niobium supported species on the catalytic dehydration of glycerol to acrolein, Appl. Catal. B-Environ. 179 (2015) 139–149.
[22] S. Chai, L. Tao, B. Yan, J.C. Vedrine, B. Xu, Sustainable production of acrolein: effects of reaction variables, modifiers doping and ZrO_2 origin on the performance of WO_3/ZrO_2 catalyst for the gas-phase dehydration of glycerol, RSC Adv. 4 (2014) 4619–4630.
[23] W. Suprun, M. Lutecki, T. Haber, H. Papp, Acidic catalysts for the dehydration of glycerol: activity and deactivation, J. Mol. Catal. A-Chem. 309 (2009) 71–78.
[24] S. Chandrasekaran, S. Ramanathan, T. Basak, Microwave food processing – A review, Food Res. Int. 52 (2013) 243–261.
[25] Q. Xie, F.C. Borges, Y. Cheng, Y. Wan, Y. Li, X. Lin, Y. Liu, F. Hussain, P. Chen, R. Ruan, Fast microwave-assisted catalytic gasification of biomass for syngas production and tar removal, Bioresour. Technol. 156 (2014) 291–296.
[26] Y. Nie, Y. Duan, R. Gong, S. Yu, M. Lu, F. Yu, J. Ji, Microwave-assisted pyrolysis of methyl ricinoleate for continuous production of undecylenic acid methyl ester (UAME), Bioresour. Technol. 186 (2015) 334–337.
[27] A. Sobhy, J. Chaouki, Microwave-assisted biorefinery, Chem. Eng. Trans. 19 (2010) 25–30.
[28] R. Luque, J.A. Menéndez, A. Arenillas, J. Cot, Microwave-assisted pyrolysis of biomass feedstocks: the way forward? Energy Environ. Sci. 5 (2012) 5481–5488.
[29] Y. Nie, Q. Xie, R. Gong, Y. Duan, S. Li, Y. Liu, X. Liang, Z. Wu, M. Lu, F. Yu, J. Ji, Method for catalytic dehydration of glycerol to acrolein, 2018.3.27, US Patent, 9, 926,253.
[30] A. Corma, Inorganic solid acids and their use in acid-catalyzed hydrocarbon reactions, Chem. Rev. 95 (1995) 559–614.
[31] T. Barzetti, E. Selli, D. Moscotti, L. Fomi, Pyridine and ammonia as probes for FTIR analysis of solid acid catalysts, J. Chem. Soc. Faraday Trans. 92 (1996) 1401–1407.
[32] C.A. Emeis, Determination of integrated molar extinction coefficients for infrared absorption bands of pyridine adsorbed on solid acid catalysts, J. Catal. 141 (1993) 347–354.
[33] F. Cavani, S. Guidetti, L. Marinelli, M. Piccinini, E. Ghedini, M. Signoretto, The control of selectivity in gas-phase glycerol dehydration to acrolein catalysed by sulfated zirconia, Appl. Catal. B-Environ. 100 (2010) 197–204.
[34] Y. Gu, S. Liu, C. Li, Q. Cui, Selective conversion of glycerol to acrolein over supported nickel sulfate catalysts, J. Catal. 301 (2013) 93–102.
[35] S. Chai, H. Wang, Y. Liang, B. Xu, Sustainable production of acrolein: gas-phase dehydration of glycerol over 12-tungstophosphoric acid supported on ZrO_2 and SiO_2, Green Chem. 10 (2008) 1087–1093.
[36] A. Alhanash, E.F. Kozhevnikova, I.V. Kozhevnikov, Gas-phase dehydration of glycerol to acrolein catalysed by caesium heteropoly salt, Appl. Catal. A-Gen. 378 (2010) 11–18.
[37] S. Chai, H. Wang, Y. Liang, B. Xu, Sustainable production of acrolein: investigation of solid acid-base catalysts for gas-phase dehydration of glycerol, Green Chem. 9 (2007) 1130–1136.
[38] A.S. de Oliveira, S.J.S. Vasconcelos, J.R. de Sousa, F.F. de Sousa, J.M. Filho, A.C. Oliveira, Catalytic conversion of glycerol to acrolein over modified molecular sieves: activity and deactivation studies, Chem. Eng. J. 168 (2011) 765–774.
[39] L. Tao, B. Yan, Y. Liang, B. Xu, Sustainable production of acrolein: catalytic performance of hydrated tantalum oxides for gas-phase dehydration of glycerol, Green Chem. 15 (2013) 696–705.
[40] S. Chai, H. Wang, Y. Liang, B. Xu, Preparation and characterization of zirconia-supported 12-tungstophosphoric acid catalyst for gas-phase dehydration of glycerol, Appl. Catal. A-Gen. 353 (2009) 213–222.
[41] Y.T. Kim, K.D. Jung, E.D. Park, Gas-phase dehydration of glycerol over ZSM-5 catalysts, Microporous Mesoporous Mater. 131 (2010) 28–36.
[42] L. Tao, S. Chai, Y. Zuo, W. Zheng, Y. Liang, B. Xu, Sustainable production of acrolein: acidic binary metal oxide catalysts for gas-phase dehydration of glycerol, Catal. Today 158 (2010) 310–316.
[43] D. Stošić, S. Bennici, S. Sirotin, C. Calais, J.L. Couturier, J.L. Dubois, A. Travert, A. Auroux, Glycerol dehydration over calcium phosphate catalysts: effect of acidic-basic features on catalytic performance, Appl. Catal. A-Gen. 447–448 (2012) 124–134.
[44] J. Deleplanque, J.L. Dubois, J.F. Devaux, W. Ueda, Production of acrolein and acrylic acid through dehydration and oxydehydration of glycerol with mixed oxide catalysts, Catal. Today 157 (2010) 351–358.
[45] I. Maetinuzzi, Y. Azizi, J. Devaux, S. Trejak, O. Zahraa, J. Leclerc, Reaction mechanism for glycerol dehydration in the gas phase over a solid acid catalyst determined with on-line gas chromatography, Chem. Eng. Sci. 116 (2014) 118–127.
[46] P. Lauriol-Garbey, G. Postole, S. Loridant, A. Auroux, V. Bellière-Beca, P. Rey, Acid-base properties of niobium-zirconium mixed oxide catalysts for glycerol dehydration by calorimetric and catalytic investigation, Appl. Catal. B-Environ. 106 (2011) 94–102.
[47] K. Omata, S. Izumi, T. Murayama, W. Ueda, Hydrothermal synthesis of W–Nb complex metal oxides and their application to catalytic dehydration of glycerol to acrolein, Catal. Today 201 (2013) 7–11.
[48] M. Massa, A. Andersson, E. Finocchio, G. Busca, F. Lenrick, L.R. Wallenberg, Performance of ZrO_2-supported Nb- and W-oxide in the gas-phase dehydration of glycerol to acrolein, J. Catal. 297 (2013) 93–109.